



# High Temperature Corrosion Behavior of Cold Spray Ni-20Cr Coating on Boiler Steel in Molten Salt Environment at 900 °C

Niraj Bala, Harpreet Singh, and Satya Prakash

(Submitted April 24, 2009; in revised form October 16, 2009)

Cold spray is an emerging technology that produces high density metallic coatings with low oxide contents and high thermal conductivity, which makes them ideal for high temperature corrosion resistance. In the current investigation, Ni-20Cr alloy powder was deposited on SA 516 boiler steel (0.19C-1.07Mn-0.020S-0.25P-0.010Si-balance Fe) by cold spray process. Oxidation kinetics was established for the uncoated and cold spray Ni-20Cr coated boiler steel in an aggressive environment of Na<sub>2</sub>SO<sub>4</sub>-60%V<sub>2</sub>O<sub>5</sub> at 900 °C for 50 cycles by the weight change technique. X-ray diffraction, FE-SEM/EDAX, and x-ray mapping techniques were used to analyze the oxidation products. Uncoated steel suffered corrosion in the form of intense spalling and peeling of its oxide scale, which may be due to the formation of unprotective Fe<sub>2</sub>O<sub>3</sub> oxides. The Ni-20Cr coating was successful in reducing the weight gain of the steel by 87.2% which may be due to the formation of oxides of nickel and chromium.

**Keywords** boiler steel, cold gas dynamic spraying, corrosion, Ni-20Cr coating

## 1. Introduction

Hot Corrosion is an accelerated form of oxidation, which occurs when the metals are heated in the temperature range of 700-900 °C, in the presence of sulfate deposits formed as a result of the reaction between sodium chloride and sulfur compounds in the gas phase around the metals (Ref 1). All the stainless steels and other common engineering alloys are attacked by fuel ash that contains vanadium with or without sulfate (Ref 2). The most common deposit found on boiler super-heaters is the sodium vanadyl vanadate, Na<sub>2</sub>O·V<sub>2</sub>O<sub>4</sub>·5V<sub>2</sub>O<sub>5</sub>, which melts at a relatively low temperature, 550 °C. Above the melting point, this ash material corrodes metals by long-term contact (Ref 3). One of the protective means to counteract the problem of hot corrosion is to coat the base material

This article is an invited paper selected from presentations at the 2009 International Thermal Spray Conference and has been expanded from the original presentation. It is simultaneously published in *Expanding Thermal Spray Performance to New Markets and Applications: Proceedings of the 2009 International Thermal Spray Conference*, Las Vegas, Nevada, USA, May 4-7, 2009, Basil R. Marple, Margaret M. Hyland, Yuk-Chiu Lau, Chang-Jiu Li, Rogerio S. Lima, and Ghislain Montavon, Ed., ASM International, Materials Park, OH, 2009.

**Niraj Bala**, Baba Banda Singh Bahadur Engineering College, Fatehgarh Sahib, Punjab, India; **Harpreet Singh**, Indian Institute of Technology Ropar, Rupnagar, Punjab, India; and **Satya Prakash**, Indian Institute of Technology, Roorkee, Uttarakhand, India. Contact e-mail: nirajbala1@rediffmail.com.

with a protective layer using various surface treatment techniques. Among the various coating methods, cold spraying is a new emerging coating technique. Cold spray process uses a high pressure, high velocity gas jet to impart the velocity for the coating particles (Ref 4). A high-pressure jet, preheated to compensate for the adiabatic cooling due to expansion, increasing the sonic velocity of the gas, heat the powder particles is expanded through a converging/diverging nozzle to form a supersonic gas jet. Powder particles, transported by a carrier gas, are injected into this gas jet. Momentum transfer from the supersonic gas jet to the particles results in high velocity particle jet. These powder particles, on impact onto the substrate surface, plastically deform and form interlinking splats, resulting in a coating (Ref 4). It has also been opined that bonding mechanism is the result of localized melting/heating due to adiabatic shear taking place due to high strain rate, high strain deformation, and rupture of the oxide film upon impact. The close metal-to-metal contact and local high temperatures create the bonding. In the cold spray process, powder particles (1-50 μm) are accelerated to velocities between 300 and 1200 m/s by the supersonic gas jet at a temperature lower than the melting temperature of the spraying material therefore providing the coating formation from particles in solid state. As a consequence, the deleterious effects of oxidation, evaporation, melting, crystallization, spallation, and other common problems in traditional thermal spray methods can be avoided (Ref 5). The Ni-base coatings are used in applications in which wear resistance combined with oxidation or hot corrosion resistance is required (Ref 6-8).

The aim of this article is to evaluate the hot corrosion performance of cold-sprayed Ni-20wt.%Cr coating on SA 516 (Grade 70) boiler steel in a simulated boiler environment of molten salt Na<sub>2</sub>SO<sub>4</sub>-60wt.%V<sub>2</sub>O<sub>5</sub> at 900 °C under cyclic conditions. The cyclic oxidation conditions

have been selected keeping in view that most of the actual industrial components work under cyclic conditions of operation.

## 2. Experimental Procedure

### 2.1 Development of Coatings

**2.1.1 Substrate Material.** The test material for the current investigation is SA 516 (Grade 70) boiler steel. The chemical composition of the material has been provided in Table 1 which presents the composition provided by supplier and the actual composition measured by spectroscopy.

**2.1.2 Coating Powder.** The commercially available Ni-20Cr powder from Sulzer Metco (US) Inc. was used as a coating material. The average particle size was 45  $\mu\text{m}$ . A SEM (scanning electron microscope) micrograph of the Ni-20Cr powder has been shown in Fig. 1. The particle shapes are of mixed type varying from spherical to elongated globules. The EDAX (energy dispersive x-ray) analysis of the powder shows Ni (79.95 wt.%) and Cr (20.5 wt.%), which is in agreement with the designated composition.

**2.1.3 Coating Formulation.** Specimens with dimensions of approximately 20 mm by 15 mm by 5 mm were prepared from the boiler steel. The specimens were polished with SiC papers down to 180 grit. Subsequently the grit blasting of the specimens was done with 60 grit

**Table 1 Chemical composition (wt.%) of SA 516 (Grade 70) boiler steel**

Chemical composition, wt.%	SA 516 (Grade 70) Boiler steel	
	Nominal composition	Actual composition
C	0.27	0.19
Mn	0.85-1.2.	1.07
P	.035 max	.25
S	.035 max	0.020
Si	0.13-0.45	0.010
Fe	Balance	Balance

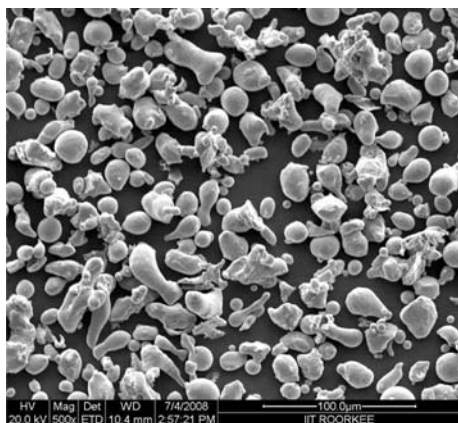


**Fig. 1** SEM micrograph of Ni-20Cr powder

(254 microns) alumina powder. Cold spray coatings were deposited at ASB Industries, Inc., Barbeton, Ohio. The system used for the coating process was Kinetics 3000 from CGT Technologies, Germany. The various parameters used during spraying are given in Table 2.

### 2.2 Characterization of the As-sprayed Coatings

X-ray diffraction (XRD) analysis of the coated samples was carried out using a Bruker AXS D-8 Advance Diffractometer (Germany) with  $\text{CuK}\alpha$  radiation and nickel filter at 20 mA under a voltage of 35 kV. The specimens were scanned with a scanning speed of 1 Kcps in the  $2\theta$  range of  $10^\circ$  to  $120^\circ$  and the intensities were recorded at a chart speed of 1 cm/min with  $2^\circ/\text{min}$  as Goniometer speed. The diffractometer interfaced with the Bruker DIFFRAC Plus x-ray diffraction software that provides the ' $d$ ' values directly on the diffraction pattern. The samples were then subjected to field emission scanning electron microscope (FE-SEM, FEI, Quanta 200F) for characterizing the surface morphology of the coatings. After the surface characterization, the samples were sectioned, mounted in epoxy powder by using hot mounting method. The mounting was done on Bainmount mounting machine, Chennai Metco Ltd, India. The mounted specimens were further subjected to polishing, using emery papers of 220, 400, 600 grit and subsequently 1/0, 2/0, 3/0, and 4/0 grades. Fine polishing was carried out to obtain a mirror finish using a 0.3  $\mu\text{m}$  diamond paste. The polished samples were characterized to obtain their cross-sectional morphology and compositions by using the FE-SEM/EDAX analysis. The EDAX Genesis software was used to calculate the composition of the elements in the coatings from their corresponding emitted x-ray peaks. Cross-sectional microhardness of the coating was measured with a load of 2.94 N using the Digital Micro Vickers Hardness tester (SHV-1000, Chennai Metco Ltd, India).

### 2.3 Molten Salt Corrosion Tests

Cyclic corrosion studies were performed in molten salt ( $\text{Na}_2\text{SO}_4$ -60%  $\text{V}_2\text{O}_5$ ) for 50 cycles. Each cycle consisted of 1 h of heating at  $900^\circ\text{C}$  in a silicon carbide tube furnace followed by 20 min of cooling at room temperature. The cyclic study provides the most severe conditions for testing and represents the actual industrial environment, where breakdown and shutdown occur frequently. A cyclic study of 50 cycles had been performed as the study of 50 cycles is considered to be adequate for attaining the steady-state

**Table 2 Process parameters for the cold spray process**

Process gas	Helium
Gun temperature	400 $^\circ\text{C}$
Gun pressure	20.5 bars
Process gas flow rate	150 $\text{m}^3/\text{s}$
Powder feed rate	40 g/min
Carrier gas	Nitrogen
Flow rate of gas	4 $\text{m}^3/\text{h}$
Coating thickness	250 $\mu\text{m}$

oxidation for the material (Ref 9-11). The studies were performed for uncoated as well as coated specimens for the purpose of comparison. The specimens were mirror polished down with 1  $\mu\text{m}$  alumina polishing on cloth wheel before the corrosion run. A coating of uniform thickness with 3 to 5  $\text{mg}/\text{cm}^2$  of  $\text{Na}_2\text{SO}_4\text{-}60\%\text{V}_2\text{O}_5$  was applied with a camel hairbrush on the preheated sample (250  $^\circ\text{C}$ ). The weight change measurements were taken at the end of each cycle with the help of an Electronic Balance machine CB-120 (Contech, Mumbai, India) having a sensitivity of  $10^{-3}$  g. The spalled scale was also included at the time of measuring weight change to determine the total rate of corrosion. Efforts were made to formulate the kinetics of corrosion. After exposure the oxidized samples were analyzed by the XRD and FE-SEM/EDAX for the surface analysis as per the procedure mentioned above. The samples were then sectioned and mounted for the cross-sectional analysis by the FE-SEM/EDAX analysis.

### 3. Results

#### 3.1 XRD Analysis of As-sprayed Coating

The XRD analysis of the cold-sprayed Ni-20Cr coating on SA 516 boiler steel in as-sprayed conditions is depicted in Fig. 2 on reduced scales. The analysis indicates the formation of Ni as a main phase along with Cr.

#### 3.2 SEM/EDAX Analysis of the As-sprayed Coating

The FE-SEM micrograph of as-sprayed Ni-20Cr coating is shown in Fig. 3(a). A higher magnification micrograph has been depicted in Fig. 3(b). The revealed microstructure consists of irregular sized particles. Some small sized particles can be observed enclosed within large crater sized particles. Some of the typical dark regions

are expected to be porosity. The particles seem to be deformed due to high impaction energy which is a characteristic of cold spray process. The elementary composition taken at the points 1 and 2 resemble the composition of the feedstock powder. Small amount of O is also found at point 2.

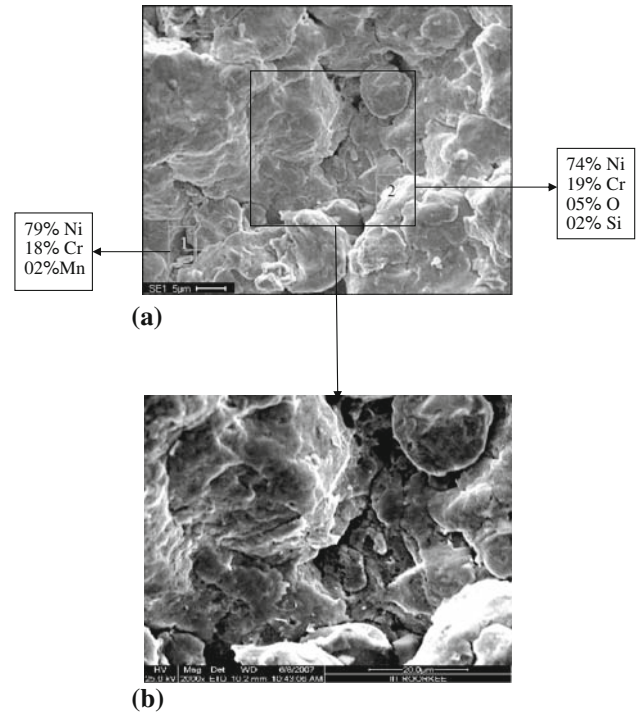


**Fig. 3** FE-SEM/EDAX analysis of SA 516 boiler steel with cold-sprayed Ni-20Cr coating showing elemental composition (wt.%) at selected points (plan view): (a) as-sprayed coating; (b) as-sprayed coating at higher magnification

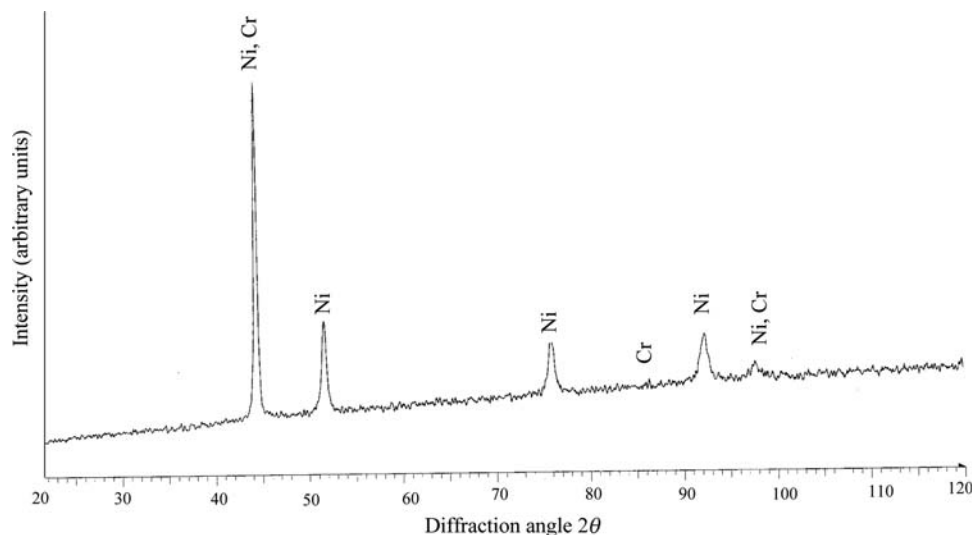


**Fig. 2** XRD pattern of cold-sprayed Ni-20Cr coating on SA 516 boiler steel in as-sprayed condition

### 3.3 Cross-sectional Analysis of the As-sprayed Coating

The cross-sectional SEM image of the cold-sprayed Ni-20Cr coating on the SA 516 boiler steel has been shown in Fig. 4. The coating has a dense appearance, in general. The coating-substrate interface is, by and large, intact and continuous, which is a characteristic feature of good adhesion between the coating and the substrate. Some

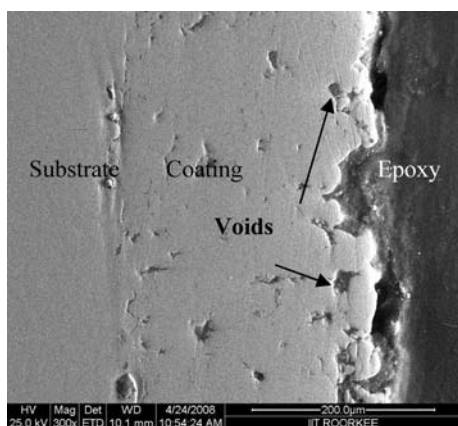


**Fig. 4** SEM micrograph along the cross section of cold-sprayed Ni-20Cr coating on SA 516 boiler steel in as-sprayed condition

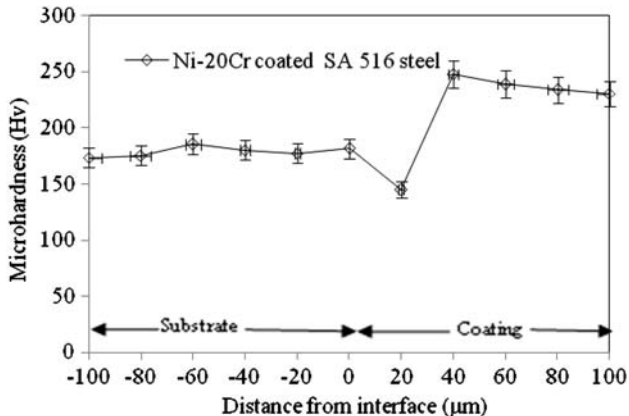


**Fig. 5** Microhardness profile of the cold-sprayed Ni-20Cr coating on SA 516 steel along the cross section

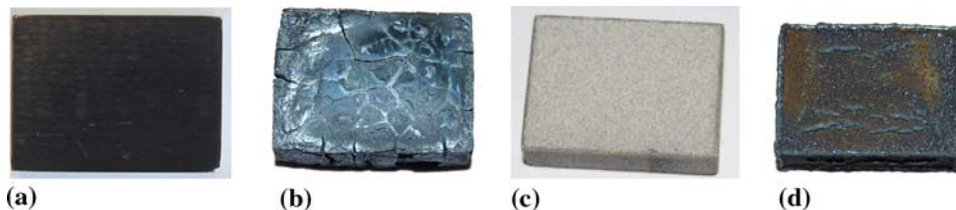


**Fig. 6** Macrographs of the uncoated and cold spray coated boiler steel samples before and after hot corrosion in  $\text{Na}_2\text{SO}_4\text{-60\%V}_2\text{O}_5$  environment at  $900^\circ\text{C}$  for 50 cycles: (a) Uncoated SA 516 steel before experimentation; (b) Uncoated SA 516 steel after experimentation; (c) Ni-20Cr-coated SA 516 steel before experimentation; (d) Ni-20Cr-coated SA 516 steel after experimentation

superficial voids could also be seen along the thickness of the coating.

### 3.4 Coating Thickness for the Coating

Average thickness of the coating has been measured from the SEM micrograph reported in Fig. 4. The average thickness as measured for the coating is  $248\ \mu\text{m}$ .

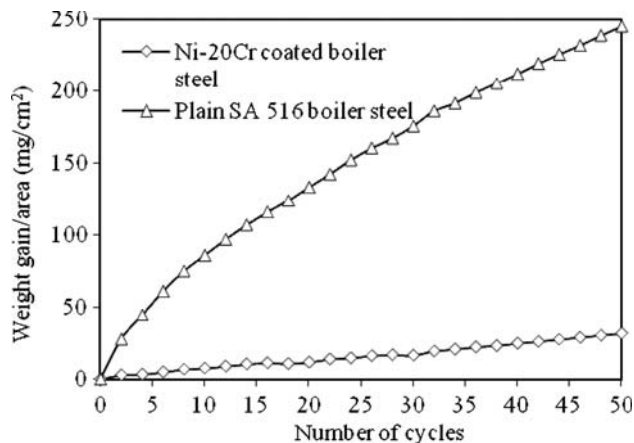


**Fig. 7** Weight change/area vs. number of cycles plot for the uncoated and cold spray Ni-20Cr-coated SA 516 steel subjected to cyclic oxidation in  $\text{Na}_2\text{SO}_4\text{-60\%V}_2\text{O}_5$  at  $900^\circ\text{C}$  for 50 cycles

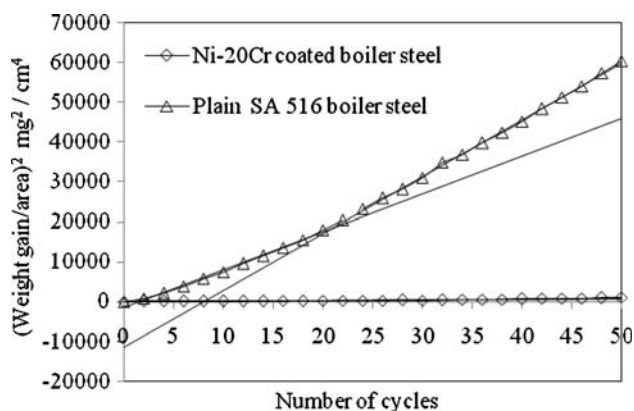


**Fig. 8**  $(\text{Weight change/area})^2$  vs. number of cycles plot for the uncoated and cold spray Ni-20Cr-coated SA 516 steel subjected to cyclic oxidation in  $\text{Na}_2\text{SO}_4\text{-60\%V}_2\text{O}_5$  at  $900^\circ\text{C}$  for 50 cycles

### 3.5 Microhardness of the As-sprayed Coating

Microhardness of the Ni-20Cr coating along with SA 516 steel substrate has been measured along the cross section. Profile for microhardness versus distance from the coating-substrate interface has been depicted in Fig. 5. Evidently, the microhardness of the coating is higher than that of the substrate steel. The microhardness values for Ni-20Cr coated steel lies in the range of 173 to 247 Hv for the substrate and the coating, with an average value, of 212.47 Hv for the coating, while the substrate steel has an average microhardness of 178.28 Hv. An unexpectedly lower value of microhardness indicated at 20  $\mu\text{m}$  from the interface may be referring to some sudden microstructural change in the coating region or small “pores” in the interface.

### 3.6 Cyclic Corrosion in Molten Salt

The macrographs of bare SA 516 and Ni-20Cr-coated SA 516 steel before experimentation have been depicted in Fig. 6(a) and (c), respectively. The macrographs of the bare, as well as, Ni-20Cr-coated SA 516 steel samples subjected to the cyclic oxidation in  $\text{Na}_2\text{SO}_4$ -60%  $\text{V}_2\text{O}_5$  at 900 °C for 50 cycles have been reported in Fig. 6(b) and (d), respectively. During the oxidation studies a fragile scale was observed on the surfaces of the uncoated SA 516 steel specimen by the end of the 6th cycle. At the end of the 9th cycle, thin flakes were found getting detached from the specimen. Exfoliation of the top scale was observed from the 14th cycle onwards. Scale cracked around 22nd cycle and there was gradual increase in the width of cracks during

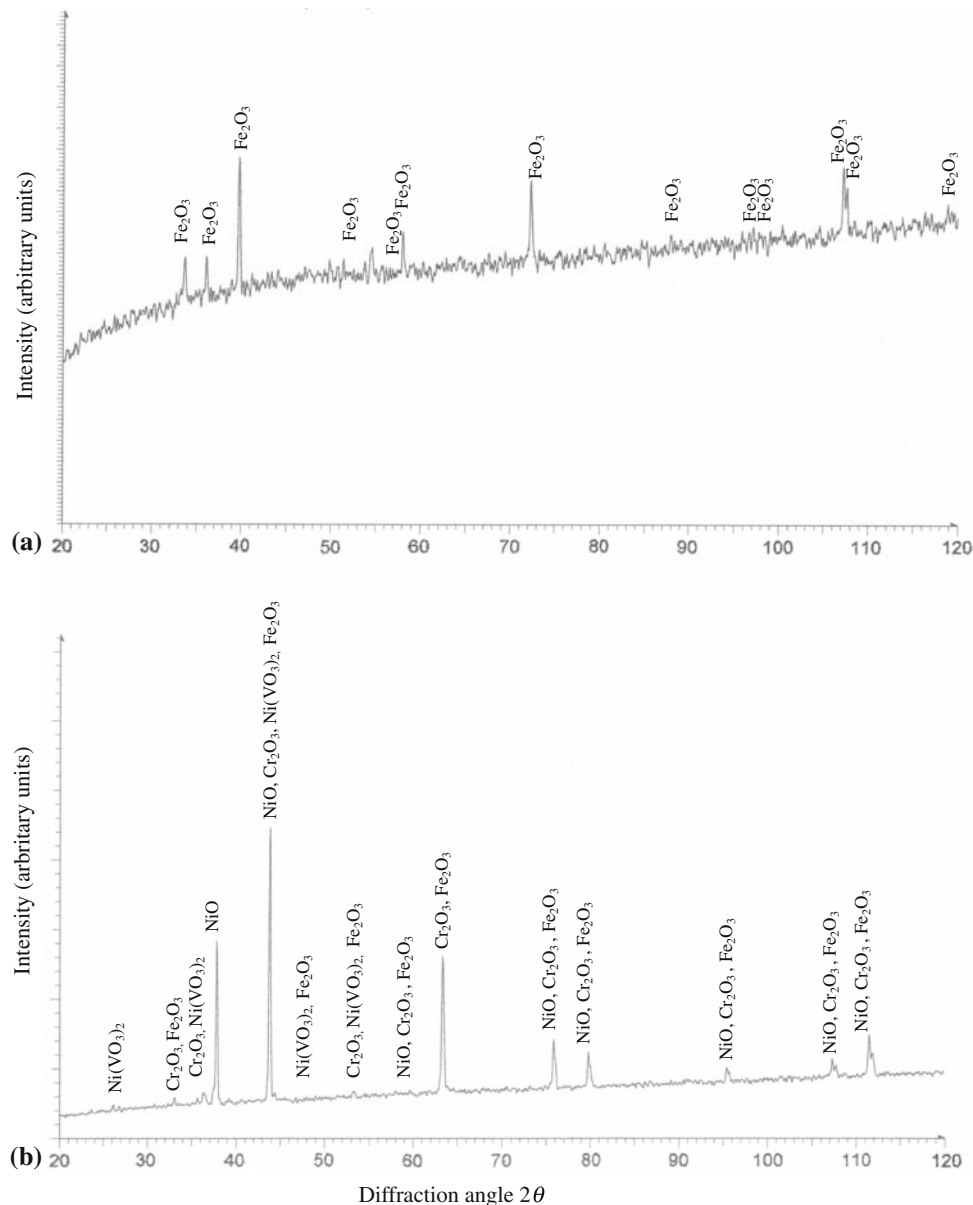


**Fig. 9** XRD patterns for the uncoated and cold spray coated steel subjected to cyclic oxidation in  $\text{Na}_2\text{SO}_4$ -60%  $\text{V}_2\text{O}_5$  at 900 °C for 50 cycles: (a) uncoated SA 516 boiler steel; (b) Ni-20Cr-coated SA 516 steel

the subsequent cycles. By the end of the 33rd cycle the specimen appeared to be swollen with cracks all over. Some material loss in powder form was also observed by the end of 38th cycle. On the other hand for the Ni-20Cr coated steel, the silver gray color of the specimen changed to gray with yellow color patches at the end of the first cycle. Some dark lines appeared on the surfaces of the specimen at the end of 14th cycle which was probably due to some oozing-out of the substrate material. At the end of 27th cycle patches of yellow color were observed on the surfaces. Subsequently, appearance of a few dots was noted on the surfaces which increased with the progress of the experiment. It is worthwhile to mention that there was no visible crack formation or spallation of the oxide scale in this case.

The weight gain plots for the uncoated and Ni-20Cr cold spray coated SA 516 steel subjected to cyclic oxidation for 50 cycles in  $\text{Na}_2\text{SO}_4$ -60% $\text{V}_2\text{O}_5$  at 900 °C are shown in Fig. 7. The uncoated steel showed continuous increase in weight gain for the entire range of exposure. Whereas the weight gain for the coated steel has shown a tendency to reach steady state with the progress of exposure time. Moreover, it is evident that weight gains have reduced significantly after the deposition of the coating. Therefore, in terms of weight gain, the Ni-20Cr coating has proved to be more corrosion resistant in the aggressive environment under study. The coating has been successful to reduce the overall weight change of the steel by 87.2%. Weight change/area squared versus the number of cycle curves for the uncoated and Ni-20Cr coated steel have been shown

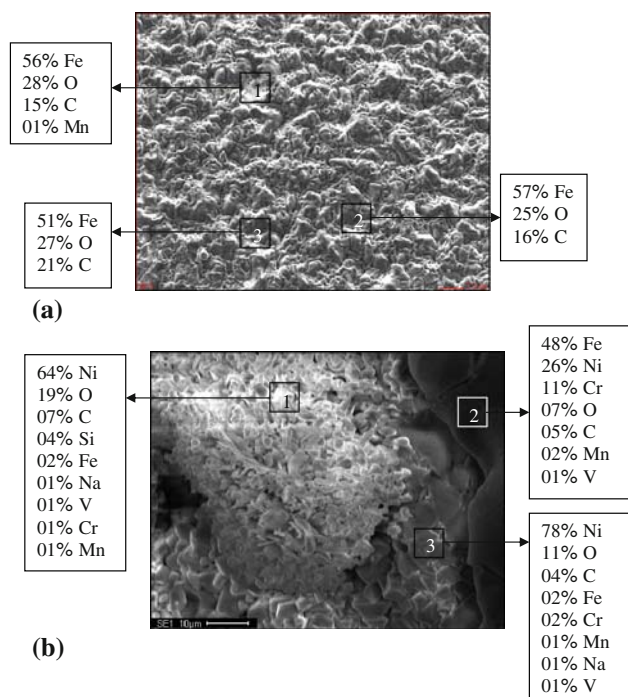


**Fig. 10** FE-SEM/EDAX analysis showing elemental composition (wt.%) for the uncoated and cold spray coated steel subjected to cyclic oxidation in  $\text{Na}_2\text{SO}_4$ -60% $\text{V}_2\text{O}_5$  at 900 °C for 50 cycles: (a) uncoated SA 516 boiler steel; (b) Ni-20Cr-coated SA 516 steel

in Fig. 8. It is evident from the trends that the parabolic rate has been followed in both the cases. However, the uncoated SA 516 steel showed some deviation from the parabolic rate law. A transition in the parabolic rate constant ( $K_p$ ) value was observed at the end of the 22nd cycle in this case. The parabolic rate constants ( $K_p$ ) were obtained from the slope of the linear regression fitted (cumulative weight gain/area)<sup>2</sup> versus number of cycles lines. The value of uncoated SA 516 steel showed a transition from  $2622 \times 10^{-10} \text{ g}^2 \text{ cm}^{-4} \text{ s}^{-1}$  after 22nd cycle to  $3947 \times 10^{-10} \text{ g}^2 \text{ cm}^{-4} \text{ s}^{-1}$ . The coated steel had the value of  $74 \times 10^{-10} \text{ g}^2 \text{ cm}^{-4} \text{ s}^{-1}$ . It is evident that the  $K_p$  value has decreased significantly after the deposition of the coating.

### 3.7 XRD Analysis of the Oxide Scales

The XRD analysis of the scale for uncoated and Ni-20Cr-coated SA 516 steel samples exposed to the hot corrosion at 900 °C for 50 cycles was done and analyzed as shown in Fig. 9.  $\text{Fe}_2\text{O}_3$  was identified as the main phase in the oxide scale of the uncoated steel after exposure (Fig. 9a). Whereas, NiO and  $\text{Cr}_2\text{O}_3$  were the main XRD phases observed in the corresponding case of Ni-20Cr-coated steel along with a few indications of  $\text{Fe}_2\text{O}_3$  phase. Peaks of  $\text{Ni}(\text{VO}_3)_2$  were also identified in the scale of the coated steel.

### 3.8 FE-SEM/EDAX Analysis

**3.8.1 Surface morphology of the scales.** The SEM micrographs indicating morphology of the uncoated and Ni-20Cr-coated steel after being subjected to the hot corrosion tests have been shown in Fig. 10. In the case of the uncoated steel (Fig. 10a), the micrograph shows a presence of uniform, dense, and rough scale. The scale in general is found to be rich in Fe and O, which provide the possibility of formation of  $\text{Fe}_2\text{O}_3$ . The SEM micrograph of the Ni-20Cr-coated steel (Fig. 10b) consists of two regions; the white region represents a granular structure and forms main part of the scale. The dark phase (oozed out material) is black in color with shiny smooth appearance. The white area indicated by point 1 consists mainly of Ni (64%), as the dominant element along with O (19%) which indicates the probable formation of NiO. C (7%), Si (4%), Fe (2%), have also been identified along with minor amounts of Na, V, Cr, and Mn. Similar composition has been indicated by area 3 which consist of Ni (78%), O (11%) as the major constituents. The dark phase which represents material oozed out of the scale has been identified by area 2, which mainly consist of as Fe (48 wt.%) and Ni (26 wt.%) along with Cr (11 wt.%) and O (17 wt.%). This indicates the diffusion of Fe from the substrate material.

**3.8.2 X-ray mappings.** Composition image (SEI) and x-ray mappings of the cross section of the uncoated SA 516 boiler steel subjected to cyclic oxidation in  $\text{Na}_2\text{SO}_4$ -60% $\text{V}_2\text{O}_5$  for 50 cycles at 900 °C are shown in Fig. 11(a). A continuous band of Fe is present in the scale. Oxygen can also be observed throughout the scale, though its concentration is more in the outer layers. V and Mn are

also distributed uniformly in the scale in a rarified manner. X-ray mappings of Ni-20Cr-coated steel (Fig. 11b) show a continuous thick band of Ni and Cr. Some patches of Fe can be observed in the outer scale and it is also present near the scale/substrate interface. Oxygen is mainly present in the outer scale in the form of patches, which are depleted of Ni and Cr.

#### 4. Discussion

The cold-sprayed Ni-20Cr coating on SA 516 boiler steel exhibited a dense morphology and was adherent to the substrate steel. The composition of the feed stock powder remained nearly same after the deposition. A minor amount of oxygen was observed by the EDAX analysis which indicates that there is only marginal possibility of formation of oxides in the coating microstructure. The microhardness varied in the range of 173 to

247 Hv with average value of 212.47 Hv. This value is significantly higher than that of the substrate steel. The bare steel showed intense spalling, peeling of the scale, and enormous weight gain. The weight gain graph (Fig. 7) shows that the weight increases continuously, although the rate of increase is high during the initial period of exposure. This rapid increase in weight gain is most likely due to the rapid diffusion of oxygen through the molten salt layer, which is identical to the results reported by Tiwari and Prakash (Ref 12) and Singh et al. (Ref 11) in their studies on the hot corrosion behavior of the Fe-based superalloy. Similar results were reported by Sidhu and Prakash (Ref 13) for plasma-sprayed Ni-20Cr coating on Gr A1 steel similar to the one under investigation. On the other hand the Ni-20Cr-coated steel has shown comparatively lesser weight gain during the course of cyclic oxidation. The coated steel has been found to be successful in reducing the weight gain by 87.2%. The coating was found to be successful in retaining its surface contact with the substrate steel during the 50 cycle experimentation as is

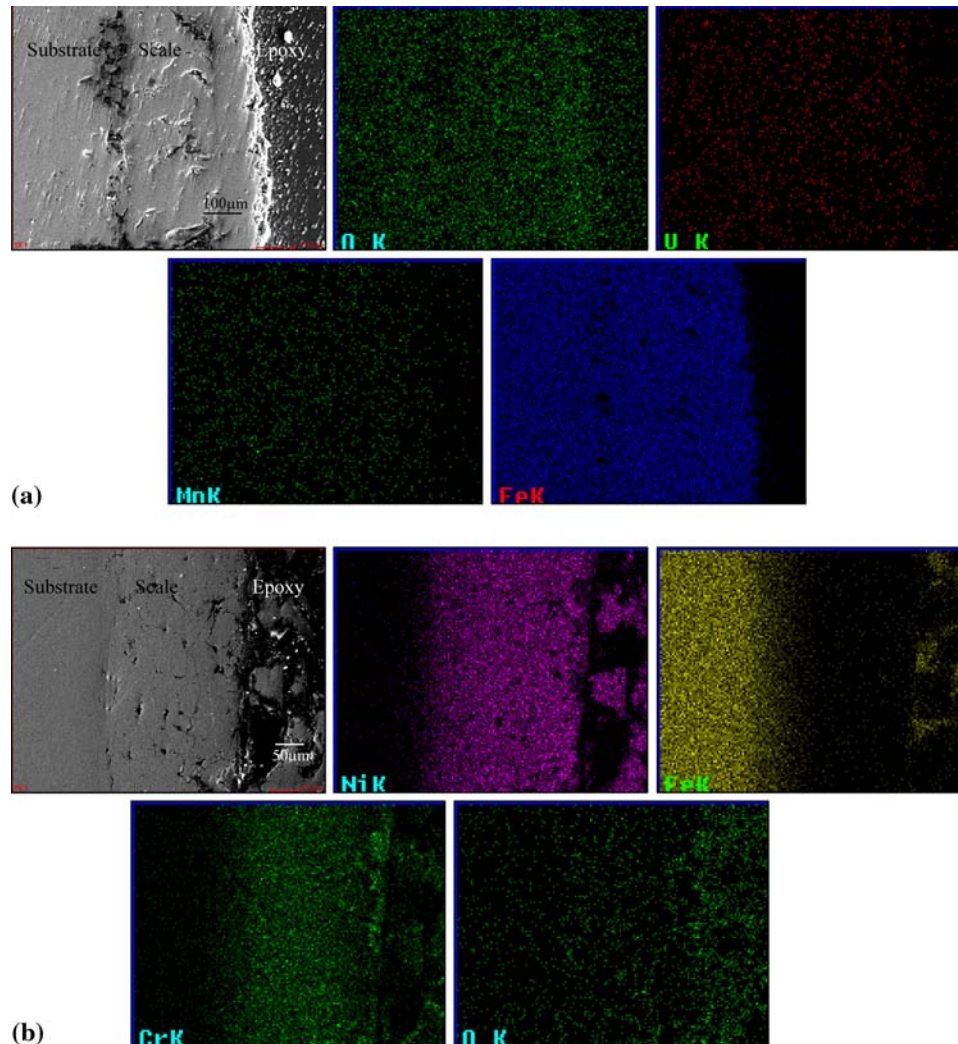
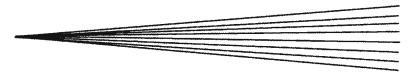


**Fig. 11** Composition image (SEI) and x-ray mapping of the cross section of the uncoated and cold spray coated SA 516 boiler steel subjected to cyclic oxidation in  $\text{Na}_2\text{SO}_4$ -60%  $\text{V}_2\text{O}_5$  at 900 °C for 50 cycles: (a) uncoated SA 516 steel; (b) Ni-20Cr-coated SA 516 steel



evident from Fig. 11(b). This shows that Ni-20Cr coating was effective in reducing the hot corrosion in the given environment. In both cases, the parabolic rate law of oxidation has been followed. However, the uncoated steel showed transition in its  $K_p$  value after 22nd cycle. Whereas, the Ni-20Cr-coated steel followed parabolic rate law up to 50th cycle, without any deviations which further indicates the protective nature of the coating.

Fe and O have been revealed as the main element in the oxide scale of the bare steel by the EDAX analysis (Fig. 10a) which indicates the possibility of formation of  $Fe_2O_3$  phase. The XRD further confirmed the formation of  $Fe_2O_3$  oxide. The same has also been observed by the x-ray mapping. The formation of  $Fe_2O_3$  has also been observed by Shi (Ref 14) during the oxidation of iron in the  $Na_2SO_4$  environment at 750 °C and by Tiwari and Prakash (Ref 15) during hot corrosion of iron-base superalloy in the  $Na_2SO_4$ -60% $V_2O_5$  environment at 900 °C. The formation of  $Fe_2O_3$  in the scale has been reported to be non-protective by Das et al. (Ref 16) during their hot corrosion study on  $Fe_3Al$ -based iron aluminide in  $Na_2SO_4$  atmosphere. The FE-SEM/EDAX analysis (Fig. 10b) of the Ni-20Cr coating shows the existence of Ni and O as the main elements in the oxide scale which provide the possibility of formation of oxides of Ni. The XRD analysis further confirmed the formation of NiO along with  $Cr_2O_3$ . The x-ray mappings also support the formation of continuous bands of Ni and Cr in the scale. The formation of NiO along with  $Cr_2O_3$  are in good agreement with the findings of Singh et al. (Ref 11), Singh (Ref 17), Longa-Nava et al. (Ref 18), Calvarin et al. (Ref 19), and Nickel et al. (Ref 20). NiO and  $Cr_2O_3$  are reported to be protective oxides by Ul-Hamid (Ref 9) and Sudararajan et al. (Ref 21). Longa-Nava et al. (Ref 18) have concluded from the studies on low-pressure plasma-sprayed Ni-20Cr coatings that the formation of chromate solute anions can prevent sulfidation of the alloy. The  $Cr_2O_3$  phase is thermodynamically stable up to 900-950 °C due to its high melting point as it forms dense, continuous, and adherent layers that inhibits interaction of oxygen with the underlying coating/substrate (Ref 22). Based on the above discussions in the present investigation, it may be concluded that the Ni-20Cr coatings can provide significant hot corrosion resistance to the boiler steel in  $Na_2SO_4$ -60% $V_2O_5$  environment. An oozing out of Fe at certain locations of the coatings as indicated by EDAX analysis has also been reported by Singh (Ref 17) on plasma-sprayed Ni-20Cr coatings and by Bala et al. (Ref 23) during their studies on cold-sprayed Ni-20Cr coatings after cyclic oxidation in air, which is an undesirable concern and needs further explanation.

## 5. Conclusion

- Cold spray process was successful in forming dense and adherent coating on SA 516 boiler steel.
- Cold spray coating of Ni-20Cr alloy powder was found to be useful in developing hot corrosion resistance in

SA 516 steel in  $Na_2SO_4$ -60% $V_2O_5$  environment at 900 °C.

- The uncoated steel showed substantial spallation of its oxide scale during hot corrosion studies in the aggressive environment of  $Na_2SO_4$ -60% $V_2O_5$  environment at 900 °C.
- The Ni-20Cr-coated steel after exposure to molten salt has shown the presence of Ni and Cr in its oxide scale, which are reported to be protective oxides.
- The Ni-20Cr coating was found to be successful in retaining its continuous surface contact with the substrate steel during the whole range of experimentation time. The oxide scales were also found to be intact.

## Acknowledgments

Harpreet Singh et al. thankfully acknowledge the research Grant from Council of Scientific and Industrial Research, New Delhi (File No. 22(0441)/07/EMR-II, dated October 23, 2007) for carrying out the R & D work on “Investigations on the role of cold spray coatings to control hot corrosion of steam generating plants.” The authors express their sincere thanks to ASB Industries, Inc., Barbeton, Ohio, USA and Guru Gobind Singh Super Thermal Power Plant, Ropar (India) for their kind co-operation during this work.

## References

1. P. Hancock, Vanadic and Chloride Attack of Superalloys, *Mater. Sci. Technol.*, 1987, **3**, p 536-544
2. K. Natesan, Corrosion-Erosion Behavior of Materials in a Coal-Gasification Environment, *Corrosion*, 1976, **32**(9), p 364-370
3. M.M. Barbooti, S.H. Al-Madfa'i, and J. Nassouri, Thermochemical Studies on Hot Ash Corrosion of Stainless Steel 304 and Inhibition by Magnesium Sulphate, *Thermochim. Acta*, 1988, **126**, p 43-49
4. J. Karthikeyan, Cold Spray Technology: International Status and USA Efforts, 2004, p 1-14
5. V.F. Kosarev, S.V. Klinkov, A.P. Alkhimov, and A.N. Papyrin, On Some Aspects of Gas Dynamics of the Cold Spray Process, *J. Therm. Spray Technol.*, 2003, **12**(2), p 265-281
6. R. Knight and R.W. Smith, HVOF Sprayed 80/20 NiCr Coatings-Process Influence Trends, *Thermal Spray: International Advances in Coatings Technology*, C.C. Berndt, Ed., May 25-June 5, 1992 (Orlando, FL), ASM International, 1992, p 159
7. M.R. Dorfman and J.A. DeBarro, Thermal Spraying: Current Status and Future Trends, Akira Ohmori, Ed., May 22-26, 1995 (Kobe, Japan), High Temperature Society of Japan, 1995, p 567
8. H. Edris, D.G. McCartney, and A.J. Sturgeon, Microstructural Characterization of High Velocity Oxy-Fuel Sprayed Coatings of Inconel 625, *J. Mater. Sci.*, 1997, **32**, p 863
9. A. Ul-Hamid, Diverse Scaling Behavior of the Ni-20Cr Alloy, *Mater. Chem. Phys.*, 2003, **80**, p 135-142
10. B.S. Sidhu and S. Prakash, Evaluation of the Corrosion Behaviour of Plasma-Sprayed  $Ni_3Al$  Coatings on Steel in Oxidation and Molten Salt Environments at 900 °C, *Surf. Coat. Technol.*, 2003, **166**, p 89-100
11. H. Singh, D. Puri, and S. Prakash, Some Studies on Hot Corrosion Performance of Plasma Sprayed Coatings on a Fe-Based Superalloy, *Surf. Coat. Technol.*, 2005, **192**, p 27-38
12. S.N. Tiwari and S. Prakash, “Studies on the Hot Corrosion Behaviour of Some Superalloys in  $Na_2SO_4$ - $V_2O_5$ ,” paper



- presented at Symposium on Localised Corrosion and Environmental Cracking (SOLCEC) (Kalpakkam, India), 1997, C-33
13. B.S. Sidhu and S. Prakash, Performance of NiCrAlY, Ni-Cr, Stellite-6 and Ni<sub>3</sub>Al Coatings in Na<sub>2</sub>SO<sub>4</sub>-60% V<sub>2</sub>O<sub>5</sub> Environment at 900 °C Under Cyclic Conditions, *Surf. Coat. Technol.*, 2006, **201**, p 1643-1654
  14. L. Shi, Accelerated Oxidation of Iron Induced by Na<sub>2</sub>SO<sub>4</sub> Deposits in Oxygen at 750 °C—A New Type Low-Temperature Hot Corrosion, *Oxid. Met.*, 1993, **40**(1-2), p 197-211
  15. S.N. Tiwari and S. Prakash, Hot Corrosion Behaviour of an Iron-Base Superalloy in Salt Environment at Elevated Temperatures, *Proceedings of the Symposium on Metals and Materials Research*, IIT, Madras, 4-5th July 1996, p 107-117
  16. D. Das, R. Balasubramaniam, and M.N. Mungole, Hot Corrosion of Fe<sub>3</sub>Al, *J. Mater. Sci.*, 2002, **37**(6), p 1135-1142
  17. B. Singh, "Studies on the Role of Coatings in Improving Resistance to Hot Corrosion and Degradation," Ph.D. Thesis, IITR, Roorkee, India, 2003
  18. Y. Longa-Nava, Y.S. Zhang, M. Takemoto, and R.A. Rapp, Hot Corrosion of Nickel-Chromium and Nickel-Chromium-Aluminum Thermal-Spray Coatings by Sodium Sulfate-Sodium Metavanadate Salt, *Corrosion*, 1996, **52**(9), p 680-689
  19. G. Calvarin, R. Molins, and A.M. Huntz, Oxidation Mechanism of Ni-20Cr Foils and its Relation to the Oxide-Scale Microstructure, *Oxid. Met.*, 2000, **53**(1-2), p 25-48
  20. H. Nickel, W.J. Quadackers, and L. Singheiser, Analysis of Corrosion Layers on Protective Coatings and High Temperature Materials in Simulated Service Environments of Modern Power Plants Using SNMS, SIMS, SEM, TEM, RBS and x-ray Diffraction Studies, *Anal. Bioanal. Chem.*, 2002, **374**, p 581-587
  21. T. Sundararajan, S. Kuroda, T. Itagaki, and F. Abe, Steam Oxidation Resistance of Ni-Cr Thermal Spray Coatings on 9Cr-1Mo Steel. Part 2: 50Ni-50Cr, *ISIJ Int.*, 2003, **43**(1), p 104-111
  22. F.H. Stott, Principles of Growth and Adhesion of Oxide Scales, *The Role of Active Elements in the Oxidation Behaviour of High Temperature Metals and Alloys*, E. Lang, Ed., Elsevier Applied Science, London, 1998,
  23. N. Bala, H. Singh, and S. Prakash, High Temperature Oxidation Studies of Cold Sprayed Ni-20Cr and Ni-50Cr Coatings on SAE 213-T22 Boiler Steel, *Appl. Surf. Sci.*, 2009, **255**(15), p 6862-6869